where the coefficients of $U_{i,j}$ and U_i are $n+1$ by n partitioned matrices. After premultiplying Eq. (9) by the transpose of $[(A-\lambda_i B)/U_i']$ the following matrix equation may be formed

$$CU_{i,j} = -EU_i \tag{10}$$

where

$$C = [A'-\lambda_i B' \vdots U_i]\begin{bmatrix} A-\lambda_i B \\ U_i' \end{bmatrix} \tag{11}$$

$$E = [A'-\lambda_i B' \vdots U_i]\begin{bmatrix} A_{,j}-\lambda_{i,j}B-\lambda_i B_{,j} \\ 0 \end{bmatrix} \tag{12}$$

where C and E are $n \times n$ matrices and $-EU_i$ is a column vector.

The derivatives of the eigenvector U_i may be found by solving the n Eqs. (10) for the components of $U_{i,j}$ after U_i and $\lambda_{i,j}$ have been substituted into Eq. (10).

Solutions to Eq. (10) may be conveniently found by decomposing matrix C into two or more matrices by means of a Choleski decomposition or some other decomposition method. The decomposed matrices would not contain derivatives; thus, if m first partial derivatives of U_i are desired with respect to m variable parameters, it is necessary to perform the decomposition only one time and then use the decomposed matrices in a forward and backward substitution scheme to solve for the components of each of the vectors $U_{i,j}$ $(j = 1, 2, \ldots, m)$.

After evaluating $\lambda_{i,j}$ and $U_{i,j}$ from Eqs. (5) and (10), respectively, their values may be substituted into Eq. (6) where the value of $\lambda_{i,jk}$ may be determined. It should be noted that only one right-hand eigenvector U_i and one left-hand eigenvector V_i is required to determine $\lambda_{i,jk}$; however, this advantage is offset somewhat by the requirement that a set of n simultaneous equations must be solved.

The second derivative of the eigenvectors may be found by differentiating Eq. (4) with respect to the kth variable parameter and rearranging the resulting expression in the form

$$\begin{aligned}(A-\lambda_i B)U_{i,jk} = &-(A_{,jk}-\lambda_{i,jk}B-\lambda_{i,j}B_{,k}- \\ &\lambda_{i,k}B_{,j}-\lambda_i B_{,jk})U_i-(A_{,j}-\lambda_{i,j}B-\lambda_i B_{,j})U_{i,k}- \\ &(A_{,k}-\lambda_{i,k}B-\lambda_i B_{,k})U_{i,j}\end{aligned} \tag{13}$$

or

$$(A-\lambda_i B)U_{i,jk} = -G \tag{14}$$

Differentiating Eq. (8) with respect to the kth parameter yields the relation

$$U_i'U_{i,jk} = -U_{i,k}'U_{i,j} \tag{15}$$

Equations (14) and (15) represent an overdetermined system of $n+1$ equations and n unknown components of $U_{i,jk}$. These equations may be written in the form

$$\begin{bmatrix} A-\lambda_i \\ U_i' \end{bmatrix} U_{i,jk} = -\begin{bmatrix} G \\ U_{i,k}'U_{i,j} \end{bmatrix} \tag{16}$$

Premultiplying Eq. (16) by the transpose of the coefficient matrix of $U_{i,jk}$ yields n simultaneous equation in n unknowns, i.e.,

$$CU_{i,jk} = -\begin{bmatrix} A-\lambda_i \\ U_i' \end{bmatrix}'\begin{bmatrix} G \\ U_{i,k}'U_{i,j} \end{bmatrix} \tag{17}$$

where the matrix C is the same as in Eq. (11). Equation (17) may be solved for $U_{i,jk}$ by using the same procedure by which Eq. (10) is solved for $U_{i,j}$ provided that all of the derivatives on the right-hand side of Eq. (13) are known.

The procedure described previously may be continued to find any order of derivative of λ_i and U_i provided the derivatives exist. The expressions for finding the derivatives of eigenvalues and eigenvectors for nonself-adjoint systems may be applied to self-adjoint systems by setting $V_i = U_i$.

References

[1] Rudisill, C. S. and Bhatia, K. G., "Optimization of Complex Structures to Satisfy Flutter Requirements," *AIAA Journal*, Vol. 9, No. 8, Aug. 1971, pp. 1487–1491.

[2] Rudisill, C. S. and Bhatia, K. G., "Second Derivatives of the Flutter Velocity and Optimization of Aircraft Structures," *AIAA Journal*, Vol. 10, No. 12, Dec. 1972, pp. 1509–1572.

[3] Wittrick, W. H., "Rates of Change of Eigenvalues, with Reference to Buckling and Vibration Problems," *Journal of the Royal Aeronautical Society*, Vol. 66, Sept. 1962, pp. 590–591.

[4] Fox, R. L. and Kapoor, M. P., "Rates of Change of Eigenvalues and Eigenvectors," *AIAA Journal*, Vol. 6, No. 12, Dec. 1968, pp. 2426–2429.

[5] Rogers, L. C., "Derivatives of Eigenvalues and Eigenvectors," *AIAA Journal*, Vol. 8, No. 5, May 1970, pp. 943–944.

[6] Plaut, R. H. and Huseyin, K., "Derivatives of Eigenvalues and Eigenvectors in Non-Self-Adjoint Systems," *AIAA Journal*, Vol. 11, No. 2, Feb. 1973, pp. 250–251.

[7] Garg, S., "Derivatives of Eigensolutions for a General Matrix," *AIAA Journal*, Vol. 11, No. 8, Aug. 1973, pp. 1191–1194.

An Experiment on an Impulse Loaded Elastic Ring

M. J. FORRESTAL* AND D. K. OVERMIER†

Sandia Laboratories, Albuquerque, N. Mex.

THE response of a circular elastic ring to a cosine distributed impulse over half the ring circumference has been the subject of analytical[1,2] and experimental[3,4] investigations. Closed form solutions for the membrane and bending stresses are presented in Ref. 2, and the experimental work reports measurements of membrane strains produced by magnetically propelled flyer plates[3] and direct magnetic pressure pulses.[4] For the flyer plate technique, energy from a capacitor bank is used to propel a thin metallic plate away from a rigid backup mass and onto the structural ring. The gap between flyer and ring is sized such that the capacitor bank is rung down before impact. However, ring deflection calculations presented in the Appendix of this Note demonstrate that the gap between ring and backup mass must also be sized to permit ring bending displacements. That is, the gap must be large enough to permit the ring to flex without hitting the backup mass. The experimental arrangement for the magnetic pressure loading technique[4] uses a rigid backup mass and does not permit free flexural motion.

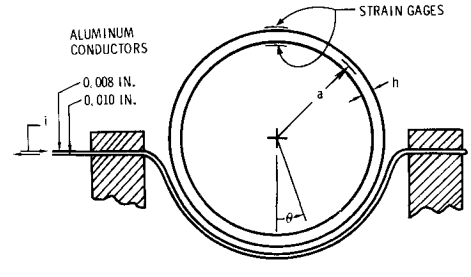

Fig. 1 Experimental arrangement.

Received October 29, 1973; revision received December 6, 1973. This work was supported by the U.S. Atomic Energy Commission. The authors thank M. J. Sagartz for helpful suggestions and E. E. Jones for performing the experiments.

Index category: Structural Dynamic Analysis.

* Division Supervisor, Shock Simulation Department. Associate Fellow AIAA.

† Staff Member, Shock Simulation Department.

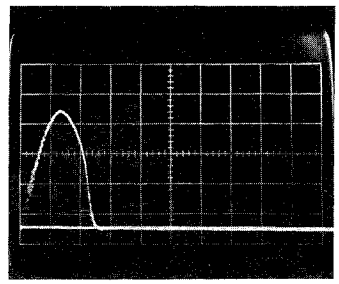

Fig. 2 Current-time; 203 ka/div, 1.0 μsec/div.

This Note presents an experimental arrangement which does not disturb flexural motion and loads the ring with a sine-squared pressure pulse which can be considered impulsive. The experimental arrangement is described, and applicability of the loading technique is demonstrated by comparing measured membrane and bending strains with predictions.

Experiment

A sketch of the experimental arrangement is shown in Fig. 1. The ring rests on two thin 1100-0 aluminum conductors (insulated from each other and the ring) which are connected to a fast-discharge capacitor bank. When the switch is closed, a magnetic pressure is generated between the conductors which is proportional to the square of the current from capacitor discharge. One conductor loads the ring, and the other plastically deforms away from the ring allowing free flexural motion. The pressure over $|\theta| < 80°$ is given by

$$p(\theta, t) = (\mu/2)[i(t)/b]^2 \cos\theta \tag{1}$$

where θ is the angular coordinate, μ is the permeability of space, b is the width of the transmission lines at $\theta = 0$, and i is the current. A sine current pulse is produced by the shaping technique described in Ref. 5, and the spatial pressure distribution is achieved by varying the width of the transmission lines.‡

One experiment is now described in detail. The 2-in.-wide ring was cut from a 12-in. O.D. by $\frac{1}{4}$-in. wall, 6061-T6 aluminum tube. The current pulse was measured with a Rogowski loop and is shown in Fig. 2; the peak impulse intensity at $\theta = 0$ as determined from the current trace is 1450 taps.§ Impulse was also measured from rigid body translation of the ring using the multiflash photographic method.[6] As shown in Fig. 3, the ring translated 3.70 in. at 50 msec and 6.45 in. at 100 msec. From Eq. (A2), the corresponding value of peak impulse intensity is 1435 taps. Thus, the current and translation measurements are in close agreement.

Strains were measured with two Micro-Measurements EP-08-125AC-350 strain gages which were mounted to the inner and outer ring surfaces at $\theta = \pi$.¶ A comparison of the measured strains and the predictions (computed for $I = 1450$ taps) given in Ref. 2 is shown in Figs. 4 and 5. The experimental membrane strain plotted in Fig. 4 is the average of the measured signals; the experimental bending strain plotted in Fig. 5 was obtained by electrically substracting the inside and outside signals. These comparisons show good correlation between measured and predicted early time membrane strain and later time bending strain.

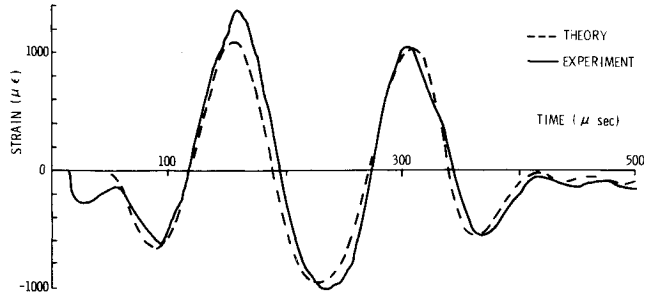

Fig. 4 Comparison of measured membrane strain with prediction.

Appendix: Ring Displacements

Solutions for the ring displacements were obtained by following the general procedures outlined in Refs. 1 and 2. These solutions are given by

$$w = \frac{Ia}{\rho ch}\left\{\frac{\sin\tau}{\pi} + \frac{1}{4(2)^{1/2}}\sin(2)^{1/2}\tau\cdot\cos\theta + \frac{\tau}{4}\cos\theta - \frac{2}{\pi}\sum_{n=2,4\ldots}^{\infty}\frac{(-1)^{n/2}\cos n\theta}{(n^2+1)^{1/2}}\left[\frac{\sin(n^2+1)^{1/2}\tau}{(n^4-1)} + \frac{n}{\alpha(n^2-1)^2}\sin\left(\frac{\alpha n(n^2-1)\tau}{(n^2+1)^{1/2}}\right)\right]\right\} \tag{A1a}$$

$$v = \frac{Ia}{\rho ch}\left\{\frac{-1}{4(2)^{1/2}}\sin(2)^{1/2}\tau\cdot\sin\theta + \frac{\tau}{4}\sin\theta + \frac{2}{\pi}\sum_{n=2,4\ldots}^{\infty}\frac{(-1)^{n/2}\sin n\theta}{(n^2+1)^{1/2}}\left[\frac{n}{n^4-1}\sin(n^2+1)^{1/2}\tau - \frac{1}{\alpha(n^2-1)^2}\cdot\sin\left(\frac{\alpha n(n^2-1)\tau}{(n^2+1)^{1/2}}\right)\right]\right\} \tag{A1b}$$

$$\tau = ct/a, \quad c^2 = E/\rho, \quad \alpha^2 = h^2/12a^2 \tag{A1c}$$

where w is radial displacement, measured positive inward; v is tangential displacement, measured positive in the θ direction; E and ρ are Young's modulus and density; h and a are shell thickness and mean radius; t is time; and I is peak intensity of impulse cosine distributed over $|\theta| < \pi/2$. These equations contain displacements due to ring deformation as well as rigid body translation. In this experimental arrangement the ring

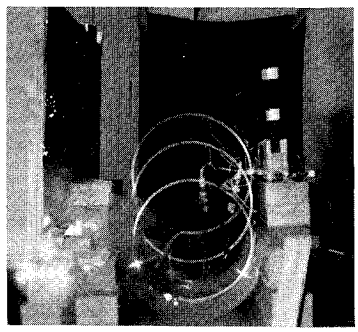

Fig. 3 Multiflash photograph of ring at $t = 0$, 50, 100 msec.

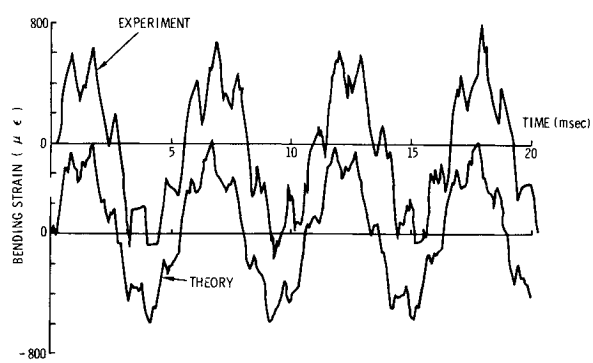

Fig. 5 Comparison of measured bending strain with prediction.

‡ Detailed discussions are presented in Ref. 3; in particular, the ring is loaded over $|\theta| \leq 80°$ rather than half its circumference.

§ 1 tap = 1 dyne-sec/cm^2.

¶ Photographs of the oscillograms are available from the authors.

translates vertically upward, and the translational motion is given by

$$y = It/4\rho h - gt^2/2 \qquad \text{(A2)}$$

where g is the acceleration due to gravity.

As discussed, the gap between ring and backup mass for a flyer plate experiment must be large enough to permit free ring deformations. For the ring used in this experiment, a set of trajectory plots of the ring displacements corresponding to several angular positions indicated that for an 80° backup mass a clearance of 0.020 in. per 1000 taps is required between the ring and the top edge of the backup mass.

References

[1] Goodier, J. N. and McIvor, I. K., "Dynamic Stability and Nonlinear Oscillations of Cylindrical Shells (Plane Strain) Subjected to Impulsive Pressure," TR 132, June 1962, Division of Engineering Mechanics, Stanford University, Stanford, Calif.

[2] Forrestal, M. J., Sagartz, M. J., and Walling, H. C., "Comment on Dynamic Response of a Cylinder to a Side Pressure Pulse," *AIAA Journal*, Vol. 11, No. 9, Sept. 1973, pp. 1355–1356.

[3] Bealing, R., "Impulse Loading of Circular Rings," *Experimental Mechanics, Proceedings of the 11th Annual Symposium*, University of New Mexico, 1971, pp. 15–26.

[4] Walling, H. C., Forrestal, M. J., and Tucker, W. K., "An Experimental Method for Impulsively Loading Ring Structures," *International Journal of Solids and Structures*, Vol. 8, 1972, pp. 825–831.

[5] Bealing, R. and Carpenter, P. G., "Exploding Foil Devices for Shaping Megamp Current Pulses," *Journal of Physics E: Scientific Instruments*, Vol. 5, 1972, pp. 889–892.

[6] Sears, F. W. and Zemanski, M. W., *University Physics*, 4th ed., Addison-Wesley, Reading, Mass., 1970, p. 49.

Unsteady Expansion Waveforms Generated by Diaphragm Rupture

J. GORDON HALL,* G. SRINIVASAN,† AND JAIPAL S. RATHI†

State University of New York at Buffalo, Buffalo, N.Y.

IN the theory of ideal shock-tube flow it is customarily assumed that the unsteady expansion wave generated by diaphragm rupture is a perfectly centered plane wave. In practice, however, such waves are generally not centered, or may not even be plane. In some experimental applications the question arises as to how to evaluate or characterize the noncentered waveform. A theoretical model for that purpose was previously introduced in an analysis of unsteady wall boundary layers within noncentered expansion or compression waves.[1,2] The present Note summarizes experimental waveform results obtained by applying the model to wall static pressure histories through expansion waves.

The expansion waves were generated by rapid bursting of a diaphragm (usually 0.003 in. thick mylar) sealing an expansion tube charged with dry room temperature air to pressure p_o (Fig. 1). The tube cross section was $1\frac{1}{2}$ in. by 5 in. The diaphragm was located at the tube end and could be preceded by a $\frac{1}{4}$-in. thick orifice plate giving critical or choked discharge to the room. Controlled initiation of the flow was achieved by electrically heating a wire taped to the stressed diaphragm. Oscilloscope records of wall static pressure vs time through the waves (Fig. 2) were obtained using three Kistler 603-A piezoelectric transducers mounted flush in the center of the 5-in. sidewall at various stations along the tube. Data were obtained to reveal the influence on waveform of orifice-plate geometry, pressure level p_o, and diaphragm material, as well as distance along the tube. Reproducibility of the experiments was extremely good in general.

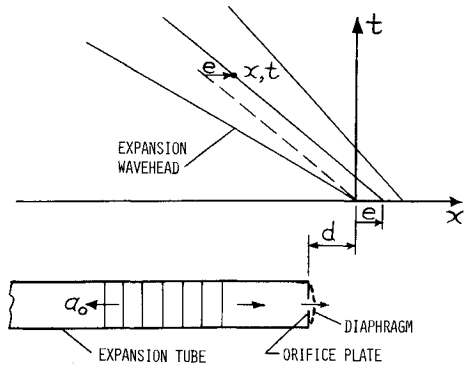

Fig. 1 Expansion tube and straight x, t characteristics for plane noncentered waves.

The theoretical model assumes a plane, isentropic simple wave with one family of the mathematical characteristics being straight lines in the distance-time or x,t plane (Fig. 1). The origin of x,t is located along the wavehead path, as described subsequently, and lies outside the tube at some distance d (typically 1 to 2 ft) from the diaphragm. This representation has no physical reality outside the tube and neglects initial three-dimensional flow effects which occur close to the diaphragm. The model also assumes that the first derivatives of the inviscid flow properties are discontinuous at the wavehead, which requires that the wave be generated with nonzero initial acceleration of the gas. The experimental waves generally had this property to a very good approximation except in the occasional instance of a poor diaphragm rupture. If the wavehead first derivatives are discontinuous it can be shown[2] that they must satisfy the relations $(\partial p/\partial t)_H = a_o(\partial p/\partial x)_H = -2\gamma p_o/(\gamma+1)t$ and $(\partial u_e/\partial t)_H = a_o(\partial u_e/\partial x)_H = -2a_o/(\gamma+1)t$. Here p = pressure, u_e = gas velocity, a = sound speed, γ = specific heat ratio (constant), and subscripts o and H denote conditions ahead of the wave (gas at rest) and at the wavehead, respectively. Thus a wavehead first derivative, such as $(\partial p/\partial t)_H$, measured at any x defines the corresponding time t from these relations and thereby uniquely locates the origin of x,t along the wavehead path. In the case of a centered wave the preceding relations apply not only at the wavehead but throughout the entire centered wave as well.

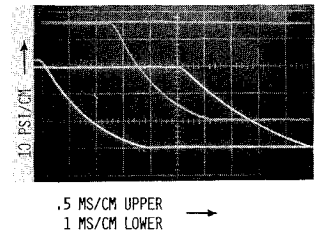

Fig. 2 Typical pressure-time oscilloscope records. Upper beam trace at 2 ft from diaphragm, 0.5 MS/cm sweep. Lower beam traces at 5 ft and 11 ft from diaphragm, 1 MS/cm sweep. p_o = 85 PSI. Choked 1″ × 5″ slot orifice.

Received October 31, 1973. This work was supported by ONR under Contract N000-14-72-C0373.

Index categories: Nonsteady Aerodynamics; Nozzle and Channel Flow.

* Professor, Department of Mechanical Engineering.

† Research Assistant.